PCCP

Accepted Manuscript

ROYAL SOCIETY OF CHEMISTRY

www.rsc.org/pccp

Journal Name

ARTICLE

Generation of stationary π-electron rotations in chiral aromatic ring molecules having non-degenerate excited states

gReceived 00th January 20xx,
Accepted 00th January 20xx

DOI: 10.1039/x0xx00000x

www.rsc.org/

Masahiro Yamaki,[a] Yoshiaki Teranishi,[b*] Hiroki Nakamura,[a] Sheng Hsien Lin,[a] and Yuichi Fujimura[a, c*]

Electron angular momentum is a fundamental quantity of high-symmetry aromatic ring molecules and has many applications to chemistry such as molecular spectroscopy. Stationary angular momentum or unidirectional rotation of π electrons is generated by excitation of a degenerated electronic excited state by a circularly-polarized photon. For low-symmetry aromatic ring molecules having non-degenerate states, such as chiral aromatic ring molecules, on the other hand, whether stationary angular momentum can be generated or not was uncertain and was not clarified so far. We have found by both theoretical treatments and quantum optimal control (QOC) simulations that a stationary angular momentum can be generated even from a low-symmetry aromatic ring molecule. The generation mechanism can be explained in terms of the creation of a dressed-state, and the maximum angular mometum is generated by the dressed state with the equal contribution from the relevant two excited states in a simple three-electronic state model. The dressed state is formed by inducing selective nonresonant transitions between the ground and each excited state by two lasers with the same frequency but having different polarization directions. The selective excitation can be carried out by arranging each photon-polarization vector orthogonal to the electronic transition moment of the other transition. We have successfully analyzed the results of the QOC simulations of (*P*)-2,2'-biphenol of axial chirality in terms of the analytically determined optimal laser fields. The present finding may open new types of chemical dynamics and spectroscopy by utilizing strong stationary ring currents and current-induced magnetic fields, which are created at a local site of large compounds such as biomolecules.

[a] *Department of Applied Chemistry, Institute of Molecular Science and Center for Interdisciplinary Molecular Science, National Chiao-Tung University, Hsinchu 30010 Taiwan*
E-mail:fujimurayuichi@m.tohoku.ac.jp
[b] *Institute of Physics, National Chiao-Tung University, and Physics Division, National Center for Theoretical Sciences, Hsinchu 30010 Taiwan*
[c] *Department of Chemistry, Graduate School of Science, Tohoku University, Sendai 980-8578 Japan*

† Footnotes relating to the title and/or authors should appear here.
Electronic Supplementary Information (ESI) available: [details of any supplementary information available should be included here]. See DOI: 10.1039/x0xx00000x

Journal Name

ARTICLE

1. Introduction

π-Electron rotation is a fundamental concept in chemistry. The rotation is the origin of aromatic ring current and angular momentum and of angular momentum-induced magnetic field. This magnetic field might play an important role in analyzing the NMR spectra of compounds.[1] Recently, with advent of both laser technology[2] and theoretical treatments[3] of electron dynamics in molecules, much interest has been paid to the laser driven π-electron rotations.[4] The ring currents could give about two orders of magnitude stronger field than those induced by traditional static magnetic fields.[5] For example, it has been demonstrated by quantum model simulations that intense laser fields can generate a strong unidirectional electronic ring current in highly symmetric aromatic ring molecules such as magnesium (Mg)-porphyrin (D_{4h})[6] and benzene (D_{6h})[7]. In Mg-porphyrin, for example, a unidirectional ring current is generated by resonant excitation of doubly degenerate excited state $^1E_+$ by circularly polarized UV laser pulses.[6] The basic mechanism is the angular momentum transfer from the photon to the relevant molecule with π-electrons.[8] So far, it has been common understanding that a low-symmetry aromatic molecule cannot produce stationary angular momentum because of no degeneracy.

There are a couple of scenarios for generation of angular momentum by applying lasers: one is to force two relevant electronic states with different energies to be degenerate.[9] This, however, would need intense laser fields. Recently, it was shown that transient angular momentum can be generated even in low-symmetry aromatic ring molecules.[10,11] However, the resultant angular momentum vector changes its direction from plus to minus direction with the time constant of $\hbar/(\varepsilon_2-\varepsilon_1)$, since two quasi-degenerate states with energies ε_1 and ε_2 are coherently excited. It is a challenging issue to find a theoretical foundation for how to generate a stationary angular momentum (unidirectional ring current)[11b] in aromatic ring molecule having non-degenerate excited states. In this paper, we present a theoretical framework to realize this in aromatic molecules with low symmetry.

In the next section, we first present an analytical theory to generate a stationary angular momentum in a three-electronic -state model. The theory is based on the nonperturbative treatment of the electronic and laser interactions. Here, two linearly-polarized intense laser fields of the same frequency with relative phase difference are independently applied to two electronic transitions. An analytical formula for stationary angular momentum is derived within rotating wave approximation (RWA). The mechanism of generation of the maximum stationary angular momentum is formation of the dressed state with the equal contribution from two excited states. To investigate possibility of another mechanism of the maximum stationary angular momentum except the dressed-state mechanism, we next present quantum optimal control (QOC) approach. In principle, the QOC approach can determine the laser fields for the maximum stationary angular momentum of any electronic system. In the Results and discussion, we show the results of the QOC simulations of the generation of stationary angular momentum in (*P*)-2,2'-biphenol of C_2 symmetry and the analysis by using the analytical approach. The results of the analysis demonstrate that the stationary angular momentum created by the QOC approach is due to the formation of the dressed state. Validity of RWA is proved by comparison with the analytical results with RWA and numerical ones without RWA.

2. Theory

In this section, we present two theoretical procedures: first we describe a general procedure for generation of stationary angular momentum of a low symmetric aromatic ring molecule. The stationary angular momentum is generated by a dressed state within rotating wave approximation, and an analytical expression for the angular momentum is derived in a three-electronic state model. Next, we briefly outline a quantum optimal control (QOC) procedure to create stationary angular momentum in the three-electronic state model.

2.1. Analytical approach

Let us consider a three-electronic-state model consisting of the ground state (with energy ε_0), two excited states, $\phi_1(\varepsilon_1)$ and $\phi_2(\varepsilon_2)$ as shown in Fig. 1a. For simplicity, we omit vibrational degrees of freedom in the treatment. Vibrational effects on electronic rotations in chiral aromatic molecules have been discussed elsewhere.[12] The molecule is assumed to be fixed on a surface or in a space by using another laser pulse.[13] The total Hamiltonian of the system in the presence of two stationary laser fields ($\boldsymbol{E}_i(t)$ with i = 1 and 2) is expressed as

$$\hat{H}(t)=\hat{H}_0+\hat{V}(t)\,. \qquad (1)$$

Here, $\hat{H}_0$ is the electronic Hamiltonian of the molecule, whose Schrödinger equation is given by

$$\hat{H}_0\phi_n=\varepsilon_n\phi_n\,, \qquad (2a)$$

and $\hat{V}(t)$, the interaction between the electronic states and the laser fields, is given as

$$\hat{V}(t)=\hat{\boldsymbol{\mu}}\cdot(\boldsymbol{E}_1(t)+\boldsymbol{E}_2(t))\,, \qquad (2c)$$

in which $\hat{\boldsymbol{\mu}}$ is the dipole moment operator, and $\boldsymbol{E}_i(t)\left(=\mathbf{e}_i E_i\cos(\omega t+\delta_i)\right)$ is the electric field of linearly-

polarized stationary lasers with polarization vector $\mathbf{e}_i$, amplitude E_i, relative phase δ_i, and frequency ω.

Let now the electric field $\boldsymbol{E}_1(t)(\boldsymbol{E}_2(t))$, selectively, interact with the excited state $\phi_1(\phi_2)$ by setting $\mathbf{e}_1 \perp \boldsymbol{\mu}_{02}$ ($\mathbf{e}_2 \perp \boldsymbol{\mu}_{01}$) (See Fig. b), in which $\boldsymbol{\mu}_{01} \equiv <\phi_0|\boldsymbol{\mu}|\phi_1>$ ($\boldsymbol{\mu}_{02} \equiv <\phi_0|\boldsymbol{\mu}|\phi_2>$) is the transition moment vector between the ground state ϕ_o and excited state $\phi_1(\phi_2)$. That is, the matrix elements of Eq. (2b) are denoted as

$$V_{01}(t) = <\phi_0|\hat{V}(t)|\phi_1> = -\boldsymbol{\mu}_{01}\cdot\boldsymbol{E}_1(t)\,, \qquad (3a)$$

and

$$V_{02}(t) = <\phi_0|\hat{V}(t)|\phi_2> = -\boldsymbol{\mu}_{02}\cdot\boldsymbol{E}_2(t)\,. \qquad (3b)$$

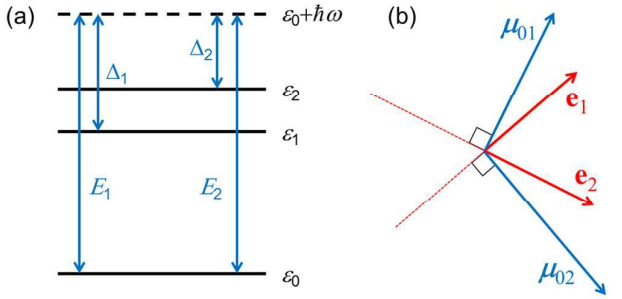

Fig. 1 (a) A three-electronic-state model for unidirectional π-electron rotation. Two linearly polarized electric fields E_1 and E_2 with the same frequency ω selectively induce nonresonant transitions between the ground state with energy ε_0 and two excited states with ε_1 and ε_2. Δ_1 and Δ_2 are detunings for the excited state ε_1 and ε_2, respectively. (b) Arrangement of photon-polarization unit vectors ($\mathbf{e}_1$ and $\mathbf{e}_2$) for the selective transitions, naturally, $\boldsymbol{\mu}_{02} \perp \mathbf{e}_1$ and $\boldsymbol{\mu}_{01} \perp \mathbf{e}_2$.

The time-dependent Schrödinger equation for the system is given in the semiclassical treatment as

$$i\hbar\frac{\partial\Phi(t)}{\partial t} = \hat{H}(t)\Phi(t)\,, \qquad (4)$$

where $\Phi(t)$ is represented in the rotating frame defined by

$$\Phi(t) = c_0(t)\phi_0\exp[-\frac{i\varepsilon_0 t}{\hbar}] + (c_1(t)\phi_1 + c_2(t)\phi_2)\exp[-\frac{i(\varepsilon_0+\hbar\omega)t}{\hbar}]\,. \quad (5)$$

Here, $\varepsilon_0 + \hbar\omega$ is taken as the energy origin in the presence of lasers. The coefficients $\{c_i(t)\}$ satisfy the normalization condition,

$$|c_0(t)|^2 + |c_1(t)|^2 + |c_2(t)|^2 = 1 \qquad .(6)$$

The time-dependent expectation value of the angular momentum operator $\hat{L} = -i\hbar\hat{l}$ [11], $L(t)$, is defined as

$$L(t) = <\Phi(t)|\hat{L}|\Phi(t)>\,. \qquad (7)$$

The time-dependent Schrödinger equation, Eq. (4) is rewritten as,

$$i\hbar\frac{d}{dt}\begin{pmatrix}c_0(t)\\c_1(t)\\c_2(t)\end{pmatrix} = \boldsymbol{H}(t)\begin{pmatrix}c_0(t)\\c_1(t)\\c_2(t)\end{pmatrix}, \qquad (8)$$

where $\boldsymbol{H}(t)$, the Hamiltonian matrix, is expressed as

$$\boldsymbol{H}(t) = \begin{pmatrix}0 & V_{01}(t)\mathrm{e}^{-i\omega t} & V_{02}(t)\mathrm{e}^{-i\omega t}\\ V_{10}(t)\mathrm{e}^{i\omega t} & \Delta_1 & 0\\ V_{20}(t)\mathrm{e}^{i\omega t} & 0 & \Delta_2\end{pmatrix}. \qquad (9)$$

To obtain an analytical expression for the expectation value of the unidirectional angular momentum, we solve Eq. (8) in the rotating wave approximation (RWA) in which the Hamiltonian matrix Eq. (9), denoted by $\boldsymbol{H}^{RWA}$, is written by omitting time-dependent terms having $\exp(\pm 2i\omega t)$ as

$$\boldsymbol{H}^{RWA} = \begin{pmatrix}0 & f_1\mathrm{e}^{i\delta_1} & f_2\mathrm{e}^{i\delta_2}\\ f_1\mathrm{e}^{-i\delta_1} & \Delta_1 & 0\\ f_2\mathrm{e}^{-i\delta_2} & 0 & \Delta_2\end{pmatrix}. \qquad (10)$$

Here, f_1 and f_2, which represent transition strengths and depend on electric field amplitude E_i, are defined as $f_1 = -\boldsymbol{\mu}_{01}\cdot\mathbf{e}_1E_1/2$ and $f_2 = -\boldsymbol{\mu}_{02}\cdot\mathbf{e}_2E_2/2$, respectively, and detunings Δ_j (j = 1, 2), which are dependent on laser frequency ω, are defined as $\Delta_1 = \varepsilon_1 - \varepsilon_0 - \hbar\omega$ and $\Delta_2 = \varepsilon_2 - \varepsilon_0 - \hbar\omega$, respectively.

Let the eigenvector of eigenvalue λ for Eq. (10) be expressed as

$$\boldsymbol{c}^\lambda = \left(c_0^\lambda, c_1^\lambda, c_2^\lambda\right) \qquad (11)$$

Here, three components are, respectively, given as

$$c_1^\lambda = \frac{f_1\mathrm{e}^{-i\delta_1}}{\lambda-\Delta_1}c_0^\lambda\,, \qquad (12a)$$

$$c_2^\lambda = \frac{f_2\mathrm{e}^{-i\delta_2}}{\lambda-\Delta_2}c_0^\lambda\,, \qquad (12b)$$

and

$$c_0^\lambda = \pm\frac{1}{\sqrt{1+\left|\frac{f_1}{\lambda-\Delta_1}\right|^2+\left|\frac{f_2}{\lambda-\Delta_2}\right|^2}}\,. \qquad (12c)$$

The corresponding eigenstate is called dressed state. We now take the three coefficients, Eqs. (12), as the initial condition. The solution of the time-dependent Schrödinger equation, Eq. (4), together with Eq. (10) can be expressed as

$$\Phi_\lambda(t) = \{c_0^\lambda\phi_0 + (c_1^\lambda\phi_1 + c_2^\lambda\phi_2)\exp(-i\omega t)\}\exp[-i\frac{(\varepsilon_0+\lambda)}{\hbar}t]\,. \qquad (13)$$

The expectation value L^λ of angular momentum operator $\hat{L}$ for Eq. (13) is expressed as

$$L^{\lambda} = <\Phi_{\lambda}(t)|\hat{L}|\Phi_{\lambda}(t)> = 2\hbar l_{12}\sin(\delta_1-\delta_2)\frac{\frac{f_1 f_2}{(\lambda-\Delta_1)(\lambda-\Delta_2)}}{1+\left|\frac{f_1}{(\lambda-\Delta_1)}\right|^2+\left|\frac{f_2}{(\lambda-\Delta_2)}\right|^2}. \quad (14)$$

Here, nonzero-matrix elements of operator $\hat{l}$ are $l_{12} = \langle\phi_1|\hat{l}|\phi_2\rangle = -l_{21}$, and the other matrix elements are zero in the three-electronic-state model.[11] The expectation value is independent of time, namely, it gives a stationary angular momentum, though the dressed state depends on time. Equation (14) simply indicates that the sign and the magnitude of L^{λ} are determined by the relative phase $\delta_1-\delta_2$ and the magnitudes of the coefficients c_1^{λ} and c_2^{λ}.

The maximum expectation value of the angular momentum is obtained when $|c_1^{\lambda}| = |c_2^{\lambda}|$ at which the maximum coherence between the two excited states is attained,

$$\frac{\lambda-\Delta_1}{f_1} = \pm\frac{\lambda-\Delta_2}{f_2}, \quad (15)$$

where positive sign is the case for the same sign of c_1^{λ} and c_2^{λ} ,while negative sign is for the opposite signs.

Using the positive sign in Eq. (15), we obtain

$$L^{\lambda} = 2\hbar l_{12}\frac{\left|\frac{f_1-f_2}{\varepsilon_2-\varepsilon_1}\right|^2}{1+2\left|\frac{f_1-f_2}{\varepsilon_2-\varepsilon_1}\right|^2}\sin(\delta_1-\delta_2). \quad (16a)$$

This can be expressed in terms of the ground state population, $|c_0^{\lambda}|^2$ as

$$L^{\lambda} = \hbar l_{12}(1-|c_0^{\lambda}|^2)\sin(\delta_1-\delta_2), \quad (16b)$$

with

$$|c_0^{\lambda}|^2 = \frac{1}{1+2\left|\frac{f_1-f_2}{\varepsilon_2-\varepsilon_1}\right|^2}. \quad (16c)$$

Equation (16b) shows that the expectation value of the angular momentum is a linear function of the ground-state population of dressed state λ, $|c_0^{\lambda}|^2$, which depends on the applied laser field amplitudes, E_1 and E_2.

Next, we determine the laser fields which give the maximum L^{λ}. From Eq.(15) with positive sign, we obtain an analytical expression for the dressed energy as

$$\lambda = \frac{f_1\Delta_2 - f_2\Delta_1}{f_1-f_2} = \frac{f_1\varepsilon_2 - f_2\varepsilon_1}{f_1-f_2} - \hbar\omega - \varepsilon_0. \quad (17)$$

The first equation in Eq. (17) can be rewritten as

$$\lambda = \frac{f_1^2 - f_2^2}{\varepsilon_2-\varepsilon_1}, \quad (18)$$

and from the second equation of Eq. (17) we have

$$\hbar\omega = \frac{f_1(\varepsilon_2-\varepsilon_0) - f_2(\varepsilon_1-\varepsilon_0)}{f_1-f_2} - \frac{f_1^2-f_2^2}{\varepsilon_2-\varepsilon_1}. \quad (19)$$

See Appendix A for brief derivation of Eqs. (18) and (19).

As is described in Appendix B, we can derive the following linear-dependent relationship between E_1 and E_2 as:

$$\mu_{01}E_2 + \mu_{02}E_1 = 0. \quad (20)$$

By using Eq. (20), we can easily obtain an analytical expression for the expectation value of the angular momentum operator in terms of E_1 or E_2. That is, we can rewrite Eq. (16a) for L^{λ} ($\equiv L$; omitting λ hereafter) in terms of E_1 as

$$L = 2\hbar l_{12}\frac{\left|\frac{(\mu_{01}^2+\mu_{02}^2)E_1}{\mu_{01}(\varepsilon_2-\varepsilon_1)}\right|^2}{1+2\left|\frac{(\mu_{01}^2+\mu_{02}^2)E_1}{\mu_{01}(\varepsilon_2-\varepsilon_1)}\right|^2}\sin(\delta_1-\delta_2). \quad (21)$$

Here, we note that the ground state population is expressed in terms of E_1 as

$$|c_0|^2 = \frac{1}{1+2\left|\frac{(\mu_{01}^2+\mu_{02}^2)E_1}{\mu_{01}(\varepsilon_2-\varepsilon_1)}\right|^2}. \quad (22)$$

We can also express E_1 in terms of $|c_0|^2$ as

$$|E_1|^2 = 2\left|\frac{\mu_{01}(\varepsilon_2-\varepsilon_1)}{(\mu_{01}^2+\mu_{02}^2)}\right|^2\left(\frac{1-|c_0|^2}{|c_0|^2}\right). \quad (23a)$$

Similarly, E_2 can be obtained in terms of $|c_0|^2$ as

$$|E_2|^2 = 2\left|\frac{\mu_{02}(\varepsilon_2-\varepsilon_1)}{(\mu_{01}^2+\mu_{02}^2)}\right|^2\left(\frac{1-|c_0|^2}{|c_0|^2}\right). \quad (23b)$$

That is, we can determine the absolute value of the amplitude of each optimal laser field (E_1 and E_2) once the ground state population is known.

The central frequency of laser, ω, is expressed in terms of E_1 by using Eq. (19) as

$$\hbar\omega = \frac{\mu_{01}^2(\varepsilon_2-\varepsilon_0)+\mu_{02}^2(\varepsilon_1-\varepsilon_0)}{\mu_{01}^2+\mu_{02}^2} - \frac{\mu_{01}^4-\mu_{02}^4}{4(\varepsilon_2-\varepsilon_1)\mu_{02}^2}E_1^2. \quad (24)$$

Thus, all parameters (E_1, E_2, and ω) of the two continuous-wave lasers to generate a stationary angular momentum can be determined by the electronic energy difference and the corresponding transition moments once the ground state population is given. We note in Eq. (24) that for $|\mu_{01}| = |\mu_{02}|$, $\hbar\omega$ is independent of E_1^2 and locates at the midpoint between ε_1 and ε_2, while as E_1^2 increases, $\hbar\omega$ is shifted to the upper energy side for $|\mu_{01}| < |\mu_{02}|$ and $\hbar\omega$ is shifted to the lower energy side for $|\mu_{01}| > |\mu_{02}|$.

So far we have derived an analytical expression for the expectation value of the angular momentum operator with positive sign in Eq. (15). If the negative sign in Eq. (15) is used, the laser field parameters are obtained by replacing f_2 in the already derived expressions by $-f_2$. The angular momentum with the opposite direction is attained.

In this section we have derived an expression for the expectation value of the stationary angular momentum by solving time-dependent Schrödinger equation Eq. (8) within RWA. If we explicitly solve Eq.(8) without RWA, the resultant expression describes a nonstationary angular momentum. That is, it is essential to adopt RWA in order to obtain stationary angular momentum. Validity of RWA in the calculation of angular momentum of a real chiral aromatic ring molecule is demonstrated in Results and discussion section.

2.2. Quantum optimal control approach

In the QOC procedure, we adopted the objective functional as[14, 15]

$$J(\boldsymbol{E}) = \frac{1}{T}\int_0^T dt \langle \Phi(t)|\hat{O}|\Phi(t)\rangle - \int_0^T dt \frac{|\boldsymbol{E}(t)|^2}{\hbar\alpha}, \qquad (25)$$

where $\hat{O}$, a projection operator of target state, is given as $\hat{O} = |\Phi_\kappa\rangle\langle\Phi_\kappa|$. Here, Φ_κ is the eigenfunction of an angular momentum operator $\hat{L}_\kappa$ around κ-axis. From the condition that the variation of Eq. (25) is zero, we get the optimal electric field of the laser as

$$\boldsymbol{E}(t) = -\alpha \,\mathrm{Im}\langle \Xi(t)|\hat{\boldsymbol{\mu}}|\Phi(t)\rangle, \qquad (26)$$

where α is a penalty factor to suppress the intensity of the optimal field, and $\Phi(t)$ is the time-dependent wavefunction under the appropriate initial condition, and $\Xi(t)$ is the Lagrange multiplier that satisfies

$$\left(i\hbar\frac{\partial}{\partial t} - \hat{H}(t)\right)\Xi(t) = -\frac{i\hbar}{T}\hat{O}\Phi(t), \qquad (27)$$

and the final condition $\Xi(T) = 0$.[11c]

3. Results and discussion

3.1. Results of quantum optimal control simulations

Let us first present the QOC simulation results for (*P*)-2,2'-biphenol as a typical example of a non-planar chiral aromatic ring molecule (point group of C_2). Three electronic excited states (*a*, b_1 and b_2), which were obtained by using TDDFT calculations,[11] are shown in Fig. 2a. The coordinates of (*P*)-2,2'-biphenol are defined in Fig. 2b. The molecule was assumed to be fixed on a surface or in a space by using by using another laser pulse. Two types of angular momenta, one in the *x*-direction and the other in the *z*-direction, can be generated by choosing an appropriate pair of electronic states.[11a, 11b] Penalty factor α for the optimal electric field of laser was set to $\alpha = 10^{41}\,\mathrm{Vm^{-2}C^{-1}}$.

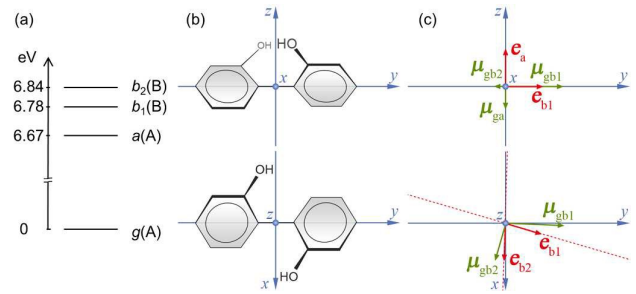

Fig. 2 (a) Electronic states and (b) geometrical structure of (*P*)-2,2'-biphenol (C_2). (c) Upper (lower): Electronic transition moments in dark green and the polarization vectors in red for two linearly polarized electric fields, E_a and E_{b1} (E_{b1} and E_{b2}) with the same frequency ω for generation of angular momentum in the *x* (*z*)-direction, L_x (L_z).

The pair of *a* and b_1 (b_1 and b_2) states generates angular momentum in the *x*- (*z*-) direction. The directions of transition dipole moments (in green) and electric fields (in red), which satisfy the conditions shown in Fig. 1b, are described in Fig. 2c. The photon polarization arrangement for the *x*-(*z*-) direction of angular momentum is shown in the upper (lower) of Fig. 2c.

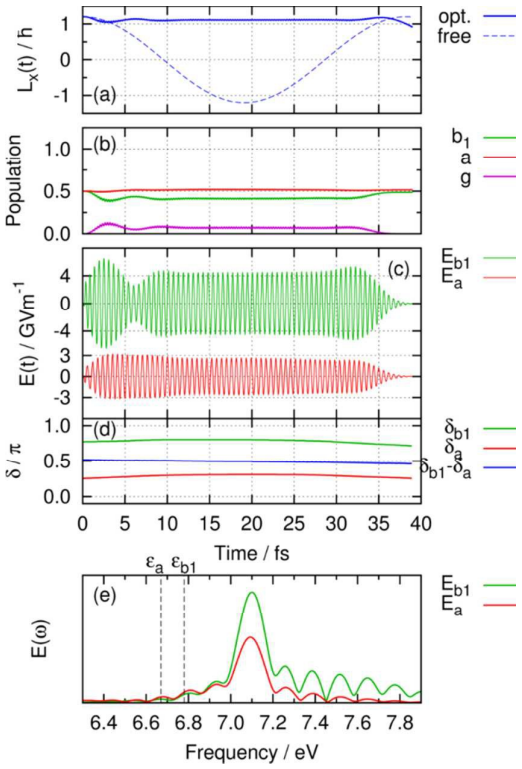

Fig. 3 Results of quantum optimal control for keeping a stationary angular momentum for (*P*)-2,2'-biphenol. (a) Angular momentum expectation value, (b) Populations of the ground state, and two excited states, *a* and b_1. (c) Electric fields of two lasers, E_{b1} and E_a. Populations of two excited states, *a* and b_1, were taken to be 0.5 as the initial condition. (d) Phases of the two electric fields, δ_{b1}, δ_a and its difference at ω = 7.1 eV as a function of time. (e) Fourier spectra of the two electric fields, $E_{b1}(t)$ and $E_a(t)$ in (c). Two broken-lines indicate the electronic energies of *a* and b_1 states.

Figure 3 presents the QOC results for keeping a stationary angular momentum in the x-direction for (*P*)-2,2'-biphenol. The molecular parameter set for (*P*)-2,2'-biphenol are $\varepsilon_a = 6.67$ eV, $\varepsilon_{b1} = 6.78$ eV and $\varepsilon_g = 0$ eV for energies and $\mu_{ag} = -1.95$ D and $\mu_{b1g} = 4.79$ D for the transition moment components projected onto the laser polarization axes.[11] $|c_g(t=0)|^2 = 0$, $|c_a(t=0)|^2 = 0.5$ and $|c_{b1}(t=0)|^2 = 0.5$ were the initial conditions. The control time *T* was tentatively set to 39 fs, which corresponds to the phase coherence time between *a* and b_1 states $\hbar/(\varepsilon_{b1} - \varepsilon_a)$. It should be noted that for much longer control time effects of vibrational motions should be taken into account.[12] Figure 3a shows the stationary angular momentum with magnitude of $L_x = 1.1\hbar$ in the *x*-direction. The target state was set to $\Phi_x = (\phi_a + i\phi_{b1})/\sqrt{2}$, whose angular momentum is in the *x*-direction.[11c] The dotted line denotes the angular momentum for no field case for comparison. The same initial condition as that for keeping a stationary angular momentum. In the latter case, we can see oscillatory behaviour with time constant of 38 fs in the angular momentum. Figure 3b shows the time dependence of the population for each electronic state. It should be noted that the populations are constant: $|c_g|^2 = 0.07$, $|c_a|^2 = 0.5$, and $|c_{b1}|^2 = 0.4$ in between around 10 and 30 fs. Figure 3c shows the electric field amplitudes for the optimal lasers, E_{b1} and E_a, which consist of two time-regions: in the first region (0 ~ 8 fs) two electric fields are nonstationary, and the corresponding angular momentum is not constant in time. In the other region after 8 fs, two electric fields are almost stationary with $|E_a|(|E_{b1}|) \cong$ 2.6 (4.5) GV/m, and with the same central frequency at ω = 7.1 eV. Here, note that the OQC approach provides the absolute value of electric field amplitude. The Fourier spectra of the two electric fields are shown in Fig. 3e. Figure 3d shows the phases of electric fields of two lasers at ω = 7.1 eV as a function of time. Time-dependence of the Fourier spectrum of electric field *E*(*t*) is evaluated by using

$$E(\omega,t) = \int d\tau \exp(i\omega\tau) w(\tau - t) E(\tau) \quad (28)$$

Here, *w*(t) is the window function, and the Beckman window function is adopted:

$$w(t) = 0.42 - 0.5\cos(\frac{2\pi t}{T}) + 0.08\cos(\frac{4\pi t}{T}) . \quad (29)$$

These are almost constant in time, and the relative phase is π/2. The resultant laser field is elliptically polarized.

3.2. Analytical approach for analysis of the QOC results

The QOC simulation results after about 8 fs in Fig. 3 indicate that the mechanism of generation of the stationary angular momentum can be explained by using the analytical theory since the two electric fields are constant, and the central frequencies are the same, and the relative phase is also constant in time. These characters of the two electric fields are the same as those adopted in the analytical approach. Let us now analyse the QOC simulation results in Fig. 3 by using the analytical expressions derived in the previous section. We need only one parameter the ground state population $|c_g|^2$ to determine all the laser parameters, ω, E_a and E_{b1}. We took $|c_g|^2 = 0.07$ from the QOC result. We got $E_a = -1.96$ GV/m and $E_{b1} = 4.80$ GV/m from Eqs. (23) and (20), and got $\hbar\omega = 7.2$ eV using Eq. (24). The dressed state energy λ =−0.51 eV was also obtained using Eq. (18). The expectation value of the angular momentum in this case becomes $L_x = 1.1\hbar$.

The comparison of the parameters determined by using the two approaches indicates that the simple analytical expressions can reproduce the optimal laser parameters between the OQC and analytical results although there are small differences in the magnitude of the amplitudes $|E_a|$ and $|E_{b1}|$. Possible origin of such differences may be setting of the initial condition for each process. The QOC simulations started with the nonstationary electronic state having the equal populations in the two excited states and zero in the ground state, and then realized the stationary dressed state with the maximum angular momentum, while the analytical treatment used the ground state population taken from the QOC simulation results.

Figure 4 shows the results of the dynamics simulations for angular momentum in the *x*-direction of (*P*)-2,2'-biphenol without using the RWA. Here, time-dependent Schrödinger equation with Hamiltonian matrix Eq. (9) was numerically solved. The initial condition, $|c_g|^2 = 0.07$, was read from the optimized result. Figure 4a exhibits constant angular momentum of 1.1ħ, which is equal to the value calculated within the RWA. The dotted curve denotes the time-dependent angular momentum for no field case.

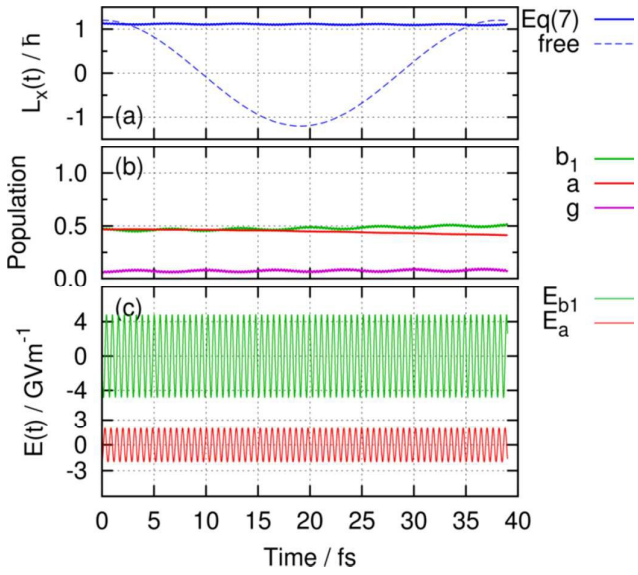

Fig. 4 Results of the dynamics simulations for (*P*)-2,2'-biphenol without RWA. (a) Angular momentum in the *x*-direction: solid line denotes the angular momentum; broken line denotes the results for no field case. (b) Populations of the ground state *g* and two excited states *a* and b_1. (c) Electric fields of two lasers E_{b1} and E_a.

Figure 4b shows nearly constant populations of the three electronic states, although weak modulations can be seen. The modulations in the population are due to the breakdown of RWA. Such a small oscillation indicates that the RWA is sufficient in the present procedure. Figure 4c shows that the electric fields, $E_a(t)$ and $E_{b1}(t)$ whose amplitudes are, respectively, $E_a = -1.96$ GV/m and $E_{b1} = 4.80$ GV/m.
The resultant laser frequency of the two lasers is $\hbar\omega = 7.20$ eV. These results are in good agreement with those evaluated in RWA, indicating the validity of the approximation.

So far we have applied our analytical treatment to generation of stationary angular momentum of L_x for (*P*)-2,2'-biphenol. Because of nonplanar structure (*P*)-2,2'-biphenol has the angular momentum component L_z as well. We can easily design the electric field lasers for L_z. The *z*-component of angular momentum is generated by three electronic states, *g*, b_1 and b_2 as shown in Fig. 2a.[11] The target eigenfunction was set as $\Phi_z = (\phi_{b1} + i\phi_{b2})/\sqrt{2}$. The laser parameters obtained were $\hbar\omega = 6.66$ eV as the central frequency, and $E_{b1} = 2.32$ GV/m and $E_{b2} = 1.54$ GV/m as the electric field amplitudes. The expectation value of *L* in the *z*-direction is $L_z = 2.75\,\hbar$. These were calculated by using the energies given in Fig. 2a and transition moment components onto the polarization axes $\mu_{b1g} = 4.79$ D and $\mu_{b2g} = 3.18$ D given in Fig. 2c. The population in the ground state $|c_g(t=0)|^2 = 0.07$ was taken as the initial condition.

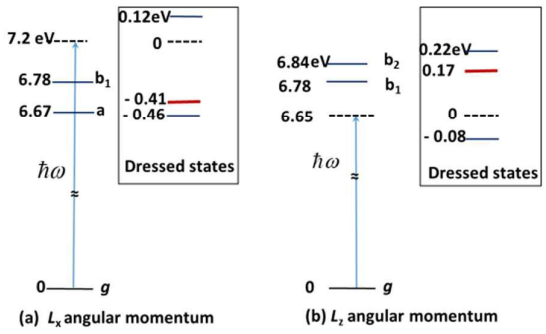

Fig. 5 Dressed states calculated by the analytical approach: (a) for the stationary angular momentum L_x; (b) for L_z. These are formed under off-resonance excitation conditions shown in left-hand side for two cases. The dressed state generating the maximum angular momentum is specified by a thick and red line for each case.

Figure 5 shows the dressed states for generation of stationary angular momentum L_x and those for L_z, which were calculated using the analytical approach. Once the dressed state λ responsible for the maximum angular momentum is determined, the other two dressed states can be calculated from the secular equation, Eq. (A1). It should be noted in Fig. 5 that the energy of the dressed state generating the maximum angular momentum locates between those of two electronic states with equal probability.

By noting that Rabi frequency ω_R is given in terms of energy difference between two dressed states $\Delta E_{dressed}$ (see Fig. 5) as $\omega_R = \Delta E_{dressed}/\hbar$, we can also recognize that the RWA is valid since Laser frequency ω is much higher than ω_R .

We also note characteristic off-resonance behaviours in the central frequency between L_x and L_z angular momentum: for L_x angular momentum the off-resonance frequency locates above the highest excited state ϕ_{b2} , while for the L_z angular momentum the off-resonance frequency locates below the lower excited state ϕ_{b1}. These off-resonance behaviours can be explained by using Eq. (24) as shown in Subsection 2.1.

It is interesting to see differences in the ground-state population between non-degenerate and degenerate cases: nonzero for the former, while zero for the latter. This can be understood from Eq. (11c). In the non-degenerate case, the ground state population can be zero only when one of the two electric fields, $f_{ag}(E_a)$ or $f_{b1g}(E_{b1})$ is infinitely strong. In other words, it is practically impossible for the ground-state population to be zero. For a degenerate case, on the other hand, the maximum angular momentum can be obtained in the case of the zero ground-state population.

4. Conclusions

In this paper, we theoretically verified that low-symmetry aromatic ring molecules, like chiral aromatic molecules, can produce a stationary angular momentum even without degenerate electronic excited states. The key point to keep a large angular momentum is to create the dressed state with the equal populations for the two excited states. This can be realized by applying two linearly-polarized stationary lasers with the same frequency and an appropriate relative phase. The two lasers independently interact with the two electronic transitions. The selective excitation can be carried out by setting each photon polarization vector orthogonal to the electronic transition moment of the other transition. Analytical expressions for the optimal lasers within RWA are derived, which have been confirmed to work well by analysing the QOC simulations for (*P*)-2,2'-biphenol.The RWA is useful for understanding the mechanism to create stationary angular momentum in aromatic ring molecules with nondegenerate electronic states. It has been shown by our simulations that the angular momentum induced by continuous wave lasers in visible and UV regions can be well reproduced within RWA. The proposed procedure for generation of an angular momentum has various kinds of application to large compounds. For example, in bio-compounds having a phenylalanine (PA) as a residue[16], the PA can act as an active site to induce conformational changes and/or chemical reaction and control these events, which can be performed by varying the magnitudes of the stationary ring currents.

Acknowledgements

Y.F. and S. H. L. thank the MOST (Research Grant MOST 104-2113-M-009-017) for financial support.

References

1 (a) T. Heine, C. Corminboeuf, and G. Seifert, *Chem. Rev.* 2005, **105**, 3889; (b) E. Steiner and P. W. Fowler, *J. Phys. Chem. A* 2001, **105**, 9553.

2 (a) E. Goulielmakis, Z. -H. Loh, A. Wirth, R. Santra, N. Rohringer, V. S. Yakovlev, S. Zherebtsov, T. Pfeifer, A. M. Azzeer, M. F. Kling, S. R. Leone, and F. Krausz, *Nature* 2010, **466**,739; (b) S. Chen, S. Gilbertson, H. Wang, M. Chini, K. Zhao, S. D. Khan, Y. Wu, and Z. Chang, *Advances in Multi-photon Processes and Spectroscopy*; World Scientific, 2011, **20**, 127.

3 (a) A. D. Bandrauk, S. Chelkowski, and H. S. Nguyen, *J. Quant. Chem.* 2004, **100**, 834; (b) P. Krause, T. Klaroth, and P. Saalfrank, *J. Chem. Phys.* 2005, **123**, 074105; (c) P. Král, T. Seideman, *J. Chem. Phys.* 2005, **123**, 184702; (d) F. Remacle, and R. D. Levine, *PNAS*, 2006, **103**, 6793; (e) L. Ulusoy and M. Nest, *J. Am. Chem. Soc*. 2011, **133**,20230; (f) K. Moore and H. Rabitz, *Nat. Chem*. 2012, **4**, 72.

4 Y. Fujimura and H. Sakai, *Electronic and Nuclear Dynamics in Molecular Systems*, World Scientific, Singapore, 2011, p. 11; references therein.

5 (a) I. Barth, C. Daniel, E. Gindensperger, J. Manz. J. F. Pèrez-Torres, A. Schild, C. Stemmle, D. Sulzer, and Y. Yang, *Advances in Multi-photon Processes and Spectroscopy*; World Scientific, 2014, **22**, 59; (b) I. Barth, J. Manz, and L. Serrano-Andrès, *Chem. Phys*. 2008, **347**, 263.

6 (a) I. Barth and J. Manz, *Angew. Chem*. 2006, **118**, 3028; (b) I. Barth and J. Manz, *Angew. Chem. Int. Ed.* 2006, **45**, 2962; (c) I. Barth, J. Manz, Y. Shigeta, and K. Yagi, *J. Am. Chem. Soc.* 2006, **128**, 7043; (d) I. Barth and J. Manz, *Progress in Ultrafast Intense Laser Science VI*, Springer 2010, p. 21.

7 K. Nobusada and K. Yabana, *Phys. Rev. A*, 2007, **75**, 032518.

8 W. Dentröder, Atoms, Molecules, and Photons: An Introduction to Atomic-, Molecular- and Quantum Physics (Graduate Texts in Physics); Springer Heidelberg, 2010, Chapt. 7.

9 To be published.

10 (a) M. Kanno, H. Kono, and Y. Fujimura, *Angew. Chem. Int. Ed.* 2006, **45**, 7995; (b) M. Kanno, K. Hoki, H. Kono, and Y. Fujimura, *J. Chem. Phys*. 2007, **127**, 204314; (c) M. Kanno, Y. Ono, H. Kono, and Y. Fujimura, *J. Phys*. *Chem*. 2012, **116**, *11260.*

11 (a) H. Mineo, M. Yamaki, Y. Teranishi, M. Hayashi, S. H. Lin, and Y. Fujimura, *J. Am. Chem. Soc.* 2012, **134**, 14279; (b) H. Mineo, S. H. Lin, and Y. Fujimura, *Chem. Phys.* 2014, **442**, 103; (c) M. Yamaki, H. Mineo, Y. Teranishi, M. Hayashi, Y. Fujimura, H. Nakamura, and H. S. Lin, *J. Phys*. *Chem. Lett*. 2014, **5**, 2044.

12 (a) M. Kanno, H. Kono, Y. Fujimura, and S. H. Lin, *Phys. Rev. Lett*. 2010, **104**,108302; (b) H. Mineo, S. H. Lin, and Y. Fujimura, *Chem. Phys.* 2014, **442**, 103.

13 (a) E. Peronme, M. D. Poulsen, C. Z. Bisgaard, and H. Stapelfeldt, *Phys. Rev. Lett.* 2003, **91**, 043003; (b) T. Kanai, S. Minemoto, and H. Sakai, *Nature* 2005, **435**, 470; (c) K. Oda, M. Hita, S. Minemoto, and H. Sakai, *Phys. Rev. Lett.* 2010, **104**, 213901.

14 (a) T. -K. Ho, H. Rabitz, and S. -I. Chu, In *Advances in Multi-photon Processes and Spectroscopy*: World Scientific, Singapore, 2015, **1**, pp. 1-57; (b) W. Zhu, J. Bonita, and H. Rabitz, *J. Chem. Phys.* 1998, **108**, 1953; (c) Y. Ohtsuki, W. Zhu, and H. Rabitz, *J. Chem. Phys.* 1999, **110**, 9825.

15 A. D. Bandrauk, *Molecules in Laser Fields*; Marcel Dekker: New York, 1994.

16 K. T. Lee, J. Sung, K. J. Lee, and S. K. Kim, *J. Chem. Phys.* 2002, **116**, 8251.

Appendix A: Derivation of Eqs.(16) and (17)

We express laser frequency ω as a function of E_1 and E_2. Dressed energy λ in Eq. (13) is a solution of the secular equation,

$$\begin{vmatrix} -\lambda & f_1\exp(i\delta_1) & f_2\exp(i\delta_2) \\ f_1\exp(-i\delta_1) & \Delta_1-\lambda & 0 \\ f_2\exp(-i\delta_2) & 0 & \Delta_2-\lambda \end{vmatrix} = 0 , \quad \text{(A1)}$$

that is,

$$\lambda = \frac{f_1^2}{\lambda-\Delta_1} + \frac{f_2^2}{\lambda-\Delta_2} , \quad \text{(A2)}$$

which is independent of $\hbar\omega$.
Using Eq. (15) we obtain

$$\lambda - \Delta_1 = \frac{\mu_{01}E_1}{\mu_{01}E_1 - \mu_{02}E_2}(\varepsilon_2-\varepsilon_1) , \quad \text{(A3a)}$$

and

$$\lambda - \Delta_2 = \frac{\mu_{02}E_2}{\mu_{01}E_1 - \mu_{02}E_2}(\varepsilon_2-\varepsilon_1) . \quad \text{(A3b)}$$

By substituting Eqs. (A3a) and (A3b) into Eq. (A2), we obtain Eq. (16). Using Eqs. (14) and (A4) we obtain Eq. (17).

Appendix B: Derivation of the equation (18)

Define an objective function for determination of optimal expectation value of angular momentum operator $\hat{L}$, $L \equiv <\Phi|\hat{L}|\Phi>$ with dressed state Φ as

$$J = E_1^{\,2} + E_2^{\,2} + \eta\{L - M\} . \quad \text{(A4)}$$

Here, M denotes the maximum value of L, and η is Lagrange multiplier under two conditions shown below,
1) $L = M$, and
2) Minimizing the intensities of the electric fields of the applied lasers as $E_1^{\,2} + E_2^{\,2}$.

$$\frac{\partial J}{\partial E_1} = 2E_1 + \eta\frac{\partial L}{\partial E_1} = 0 , \quad \text{(A5a)}$$

$$\frac{\partial J}{\partial E_2} = 2E_2 + \eta\frac{\partial L}{\partial E_2} = 0 , \quad \text{(A5b)}$$

and

$$\frac{\partial J}{\partial \eta} = L - M = 0 . \quad \text{(A5c)}$$

In Eq. (A5a),

$$\frac{\partial L}{\partial E_i} = \frac{\partial L}{\partial X}\frac{\partial X}{\partial E_i} , \quad \text{(A6)}$$

with $X \equiv \dfrac{\mu_{01}E_1 - \mu_{02}E_2}{2(\varepsilon_2-\varepsilon_1)}$,

$$\frac{\partial X}{\partial E_1} = \frac{\mu_{01}}{2(\varepsilon_2-\varepsilon_1)} , \quad \text{(A7a)}$$

and

$$\frac{\partial X}{\partial E_2} = -\frac{\mu_{02}}{2(\varepsilon_2-\varepsilon_1)} . \quad \text{(A7b)}$$

Equations (A5a) and (A5b) are re-expressed as

$$\frac{\partial J}{\partial E_1} = 2E_1 + \frac{\mu_{01}}{2(\varepsilon_2-\varepsilon_1)}\frac{\partial L}{\partial X} = 0 , \quad \text{(A8a)}$$

and

$$\frac{\partial J}{\partial E_2} = 2E_2 - \frac{\mu_{02}}{2(\varepsilon_2-\varepsilon_1)}\frac{\partial L}{\partial X} = 0 . \quad \text{(A8b)}$$

From Eqs. (A8a) and (A8b), we obtain Eq. (18).